Structural Engineering and Mechanics, Vol. 41, No. 6 (2012) 751-758
DOI: http://dx.doi.org/10.12989/sem.2012.41.6.751

Locating a weakened interface in a laminated elastic plate

J. Zhu[1], J.S. Yang[2] and W.Q. Chen[3,4]*

[1]*Department of Civil Engineering, Zhejiang University, Zijingang Campus, Hangzhou 310058, China*
[2]*Department of Engineering Mechanics, University of Nebraska, Lincoln, NE 68588-0526, USA*
[3]*State Key Lab of CAD & CG, Zhejiang University, Zijingang Campus, Hangzhou 310058, China*
[4]*Department of Engineering Mechanics, Zhejiang University, Yuquan Campus, Hangzhou 310027, China*

(Received March 8, 2011, Revised February 6, 2012, Accepted February 21, 2012)

Abstract. We study thickness-shear (TSh) free vibrations of an unbounded, laminated elastic plate with three layers of different materials. One of the two interfaces is slightly weakened as described by the shear-lag model that allows the displacement to be discontinuous across the interface. A frequency equation is obtained from the linear theory of elasticity. A perturbation solution of the frequency equation is obtained from which the frequency shifts of TSh modes due to the weakened interface can be calculated. It is shown that the frequency shifts of TSh modes of different orders are different, and they satisfy different conditions when different interfaces are weakened. These conditions are obtained which can potentially be used as criteria for determining specifically which interface is weakened.

Keywords: locating; thickness-shear; laminated elastic plate; TSh modes; weakened interface; frequency shifts

1. Introduction

Laminated elastic plates are widely used in various engineering structures, airplanes, and vehicles (Piskunov and Rasskazov 2002, Reddy 2004). Failure of these structures often begins with local weakening of an interface in the laminates. The weakened and damaged interfaces (including delamination and interlayer slip, as limiting cases) will degrade the integrity of the laminated structures in general. Thus, a lot of research effort has been made to investigate the effect of bonding imperfections on the static, dynamic and thermal responses as well as buckling of elastic laminated structures (Lu and Liu 1992, Tomar and Gogna 1995, Cheng *et al*. 1996, Di Sciuva 1997, Icardi 1999, Librescu and Schmidt 2001, Cheng and Batra 2001, Shu 2001, Chen *et al*. 2003, Chen *et al*. 2004, Chen *et al*. 2005, Fan *et al.* 2006, Kim and Lee 2007, Li *et al.* 2007, Wang *et al.* 2008, Kumar and Singh 2009, Wang *et al.* 2010). These direct analyses are very important for us to gain a comprehensive understanding of the behavior of damaged structures. In practice, the inverse analysis is also important for the purpose of structural health monitoring (Friswell and Mottershead 2001, Friswell 2007). In particular, how to locate a specific weak interface in a laminated plate is

*Corresponding author, Professor, E-mail: chenwq@zju.edu.cn

fundamental to the strength and safety consideration of laminated structures. At present it is not difficult to determine which area of a laminated plate has a weak interface (Chen *et al*. 1998, Yang *et al*. 2001, Rinker *et al*. 2003), but how to locate the specific weak interface when there are two or more interfaces remains a challenging problem.

This paper attempts to locate a specific weak interface in a laminated plate using TSh or antiplane or shear-horizontal (SH) vibration modes of different orders. The weak interface is described by the so-called shear-lag model (Cheng *et al*. 1996, Di Sciuva 1997, Icardi 1999, Librescu and Schmidt 2001, Cheng and Batra 2001, Jin *et al*. 2005, Yang *et al*. 2006) that allows the interface shear displacement to be slightly discontinuous. Such a weak interface causes the TSh resonant frequencies of the laminate to be different from a perfectly bonded laminate without a weak interface. Since TSh modes of different orders have different displacement profiles along the plate thickness, these modes feel a weak interface at a specific location differently, with different frequency shifts. Therefore it seems possible to use different frequency shifts of different modes to determine which specific interface is weakened.

2. Governing equations and fields

Consider the three-layered elastic plate in Fig. 1. The layers are of isotropic materials. We discuss the first (top) layer in detail. The two other layers are similar. For isotropic layers the so-called SH motions described by the following displacement field are allowed by the linear theory of elasticity

$$u_1 = u_2 = 0, \quad u_3 = u(x_2, t) \tag{1}$$

Eq. (1) is for specialized, x_1-independent antiplane motions called TSh modes in a plate. The only equation of motion for TSh modes is

$$T_{23,2} = \rho_1 \ddot{u} \tag{2}$$

where ρ_1 is the mass density. The relevant shear stress component is related to the displacement gradient through the following constitutive relation

$$T_{23} = c_1 u_{,2} \tag{3}$$

where c_1 is the shear modulus of the material. Substitution of Eq. (3) into Eq. (2) yields the displacement equation of motion

$$c_1 u_{,22} = \rho_1 \ddot{u} \tag{4}$$

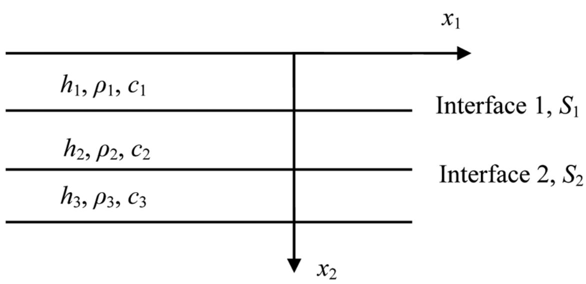

Fig. 1 A three-layered plate with weak interfaces

It is straightforward to verify that for time-harmonic motions with an $\exp(i\omega t)$ time factor the general solution to Eq. (4) is

$$u = A_1 \sinh k_1 x_2 + B_1 \cosh k_1 x_2 \tag{5}$$

where A_1 and B_1 are undetermined constants, and

$$k_1 = i\sqrt{\frac{\rho_1}{c_1}}\omega \tag{6}$$

From Eq. (3), the shear stress corresponding to Eq. (5) takes the following form

$$T_{23} = c_1 k_1 (A_1 \cosh k_1 x_2 + B_1 \sinh k_2 x_2) \tag{7}$$

which will be needed for boundary and interface conditions. For the second and the third layers, the displacement and stress fields are similar to Eqs. (5) and (7), with material constants and undetermined constants associated by subscripts 2 and 3, respectively.

3. Boundary and interface conditions

At the top and bottom of the plate and the two interfaces we prescribe the following boundary and interface conditions

$$T_{23}(0) = 0 \tag{8}$$

$$T_{23}(h_1)^+ = T_{23}(h_1)^- = K_1[u(h_1)^+ - u(h_1)^-] \tag{9}$$

$$T_{23}(h_1+h_2)^+ = T_{23}(h_1+h_2)^- = K_2[u(h_1+h_2)^+ - u(h_1+h_2)^-] \tag{10}$$

$$T_{23}(h_1+h_2+h_3) = 0 \tag{11}$$

where "+" and "–" as superscripts represent upper and lower limits. Eqs. (8) and (11) are traction-free boundary conditions at the top and bottom of the plate. Eqs. (9) and (10) are according to the shear-lag interface model with which the shear stress is continuous at an interface but the displacement is allowed to have a discontinuity (Chen *et al.* 1996). In the shear-lag interface model the thickness of the interface is treated as zero. K is the effective interface elastic stiffness that describes how well the two materials are bonded. $K = \infty$ is for perfect bonding with continuous displacement. Physically, we may think the interface as a separate phase with a very small thickness 2δ, in which the shear strain can be considered as uniform along the thickness direction. Since for TSh mode, the shear strain is calculated as $S_{23} = u_{,2}$, the shear stress of the interface without neglecting thickness can be approximately written as

$$T_{23} = c\frac{u(\delta) - u(-\delta)}{2\delta} \tag{12}$$

where c is the usual shear modulus of the interface material, and $[u(\delta) - u(-\delta)]/2\delta$ is the approximate shear strain, which is obtained by replacing the differentiation by the difference. Comparing Eq. (12) with Eqs. (9) or (10) we can identify the relation between the real interface shear modulus c and the effective interface shear modulus K as $c = 2\delta K$. Therefore K in fact represents a combination of the interface elasticity and thickness. We note that Eqs. (9) and (10) in fact each represents two conditions. Therefore Eqs. (8)-(11) together are six conditions.

4. Frequency equation

For later convenience, we introduce the interface effective compliance by

$$S_1 = 1/K_1, \quad S_2 = 1/K_2 \tag{13}$$

Substituting Eqs. (5), (7) and similar expressions of the second and the third layers into Eqs. (8)-(11), we obtain six linear and homogeneous equations for A_1 through A_3 and B_1 through B_3. For nontrivial solutions the determinant of the coefficient matrix of these equations has to vanish, which gives the following frequency equation that determines the free vibration resonant frequency ω

$$F(\omega) + G(\omega)S_1 + H(\omega)S_2 + J(\omega)S_1S_2 = 0 \tag{14}$$

where

$$F(\omega) = N_1N_4N_6k_3c_3 + N_2N_3N_6k_2c_2 + (N_1N_3N_5k_3c_3 + N_2N_4N_5k_2c_2)k_1c_1/k_2c_2 \tag{15}$$

$$G(\omega) = (N_1N_4k_3c_3 + N_2N_3k_2c_2)N_5k_1c_1 \tag{16}$$

$$H(\omega) = (N_3N_6k_2c_2 + N_4N_5k_1c_1)N_1k_3c_3 \tag{17}$$

$$J(\omega) = N_1N_3N_5k_1c_1k_2c_2k_3c_3 \tag{18}$$

and

$$N_1 = \exp(k_3h_3) - \exp(-k_3h_3) \tag{19}$$

$$N_2 = \exp(k_3h_3) + \exp(-k_3h_3) \tag{20}$$

$$N_3 = \exp(k_2h_2) - \exp(-k_2h_2) \tag{21}$$

$$N_4 = \exp(k_2h_2) + \exp(-k_2h_2) \tag{22}$$

$$N_5 = \exp(k_1h_1) - \exp(-k_1h_1) \tag{23}$$

$$N_6 = \exp(k_1h_1) + \exp(-k_1h_1) \tag{24}$$

Eq. (14) determines a series of resonant frequencies $\omega_{(n)}$, with $n = 1, 2, \ldots$.

5. Frequency shifts due to a weak interface

An interface with nearly perfect bonding is represented by a small S. In this section we consider these slightly weakened interfaces. First we denote the resonant frequencies when both interfaces are perfectly bonded ($S_1 = S_2 = 0$) by $\overset{0}{\omega}_{(n)}$ which satisfies $F(\overset{0}{\omega}_{(n)}) = 0$. Although our ultimate goal is to determine the specific weak interface when there is only one such weak interface, we begin with the situation when both interfaces are slightly weakened (both S_1 and S_2 are nonzero and small) and denote the resonant frequencies perturbed by the weak interfaces by $\omega_{(n)} = \overset{0}{\omega}_{(n)} + \Delta\omega_{(n)}$, where $\Delta\omega_{(n)}$ is small. Then, to the first order of $\Delta\omega_{(n)}$, from the frequency equation in Eq. (14), we obtain, approximately

$$\Delta\omega_{(n)} \cong -\frac{G(\overset{0}{\omega}_{(n)})}{F'(\overset{0}{\omega}_{(n)})}S_1 - \frac{H(\overset{0}{\omega}_{(n)})}{F'(\overset{0}{\omega}_{(n)})}S_2 \tag{25}$$

Eq. (25) shows that modes of different orders (different values of n) feel the weakened interfaces differently, with different frequency shifts. In the special case when there is only one weak interface, e.g., the upper interface ($S_1 \neq 0, S_2 = 0$), Eq. (25) reduces to

$$\Delta\omega_{(n)} \cong -\frac{G(\overset{0}{\omega}_{(n)})}{F'(\overset{0}{\omega}_{(n)})}S_1 \tag{26}$$

Let m be an integer different from n. Corresponding to m, we can also write

$$\Delta\omega_{(m)} \cong \frac{G(\overset{0}{\omega}_{(m)})}{F'(\overset{0}{\omega}_{(m)})}S_1 \tag{27}$$

We can eliminate S_1 from Eqs. (26) and (27). This results in the following relationship between the frequency shifts of two different modes corresponding to m and n

$$\frac{\Delta\omega_{(n)}}{\Delta\omega_{(m)}} \cong \frac{G(\overset{0}{\omega}_{(n)})}{F'(\overset{0}{\omega}_{(n)})} \bigg/ \frac{G(\overset{0}{\omega}_{(m)})}{F'(\overset{0}{\omega}_{(m)})} \tag{28}$$

Eq. (28) is a condition on the frequency shifts of the nth and the mth modes when the upper interface is weakened and the lower interface is perfect. Similarly, if the lower interface is weakened and the upper interface is perfect ($S_1 = 0, S_2 \neq 0$), we have

$$\Delta\omega_{(n)} \cong -\frac{H(\overset{0}{\omega}_{(n)})}{F'(\overset{0}{\omega}_{(n)})}S_2 \tag{29}$$

$$\Delta\omega_{(m)} \cong -\frac{H(\overset{0}{\omega}_{(m)})}{F'(\overset{0}{\omega}_{(m)})}S_2 \tag{30}$$

$$\frac{\Delta\omega_{(n)}}{\Delta\omega_{(m)}} \cong \frac{H(\overset{0}{\omega}_{(n)})}{F'(\overset{0}{\omega}_{(n)})} \bigg/ \frac{H(\overset{0}{\omega}_{(m)})}{F'(\overset{0}{\omega}_{(m)})} \tag{31}$$

We propose to use Eqs. (28) and/or (31) to determine the specific weak interface when there is only one weak interface. The procedure begins with the choice of two modes, i.e., the specification of n and m. The corresponding resonant frequencies when the interfaces are both perfect can be obtained from solving $F(\overset{0}{\omega}_{(n)}) = 0$. Then the right-hand sides of Eqs. (28) and (31) are known. $\Delta\omega_{(n)}$ and $\Delta\omega_{(m)}$ are obtained from experimental measurement. If they satisfy Eq. (28), the upper interface is weak. If they satisfy Eq. (31), the lower interface is weak.

6. Numerical results

For a numerical example, consider the case when the two outer plates are AlN with density

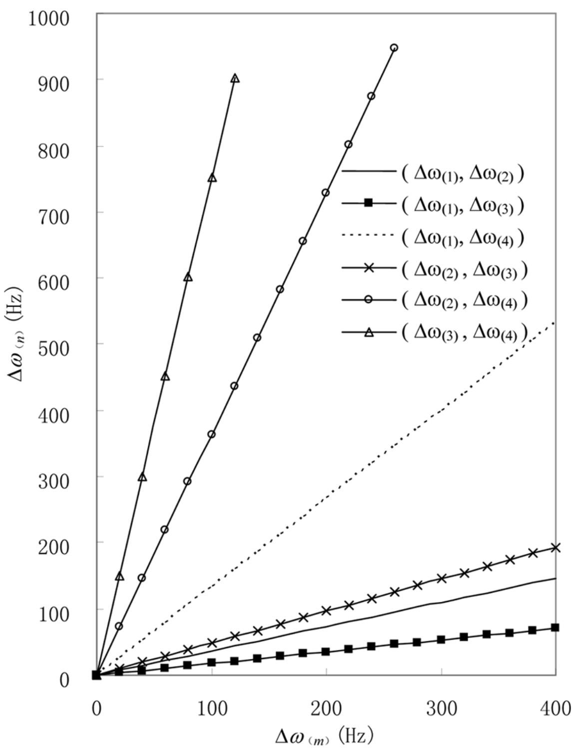

Fig. 2 Relations among frequency shifts of different modes when Interface 1 is weakened

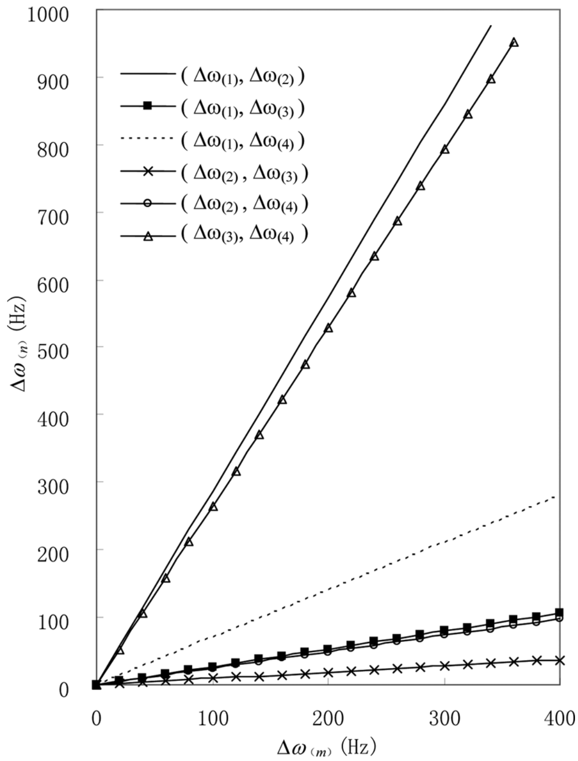

Fig. 3 Relations among frequency shifts of different modes when Interface 2 is weakened

$\rho_1 = \rho_3 = 5665$ kg/m^3 and shear modulus $c_1 = c_3 = 4.23 \times 10^{10}$ Pa (Tsubouchi *et al.* 1981), and the middle layer is SiO_2 with $\rho_2 = 2200$ kg/m^3 and $c_2 = 3.1 \times 10^{10}$ Pa (Accuratus Corporation 2012). $h_1 = 0.6$ mm, $h_2 = h_3 = 1.2$ mm. In the numerical calculation, both S_1 and S_2 are assumed to be the order of 10^{-17} m^3/N. With such values, the frequency shifts calculated from the approximate expression, Eq. (25), are almost the same as that from the exact expression, Eq. (14). In such a situation, the interface can be considered as slightly weakened, since the weakness almost doesn't affect the dynamic behavior. With the increase of interface effective compliance, however, the first-order approximation of Eq. (14) based on Taylor's expansion may become insufficient, and Eq. (25) will no longer be valid.

Eqs. (28) and (31) are plotted in Figs. 2 and 3, respectively. For the plate considered in the numerical example, with its thickness being of the order of millimeters, the resonant frequencies ($\sim\sqrt{c/\rho h^2}$) are of the order of MHz. The frequency shifts are found to be of the order of 10^2 to 10^3 Hz for the chosen values of S (of the order of 10^{-17} m^3/N). These frequency shifts are considered as clear signals in millimeter-sized acoustic wave devices or structures, and can be easily measured by appropriate existing techniques. As we can see from Figs. 2 and 3, the ratios of frequency shifts for different modes almost keep constants when the interface is slightly imperfect, and the slopes can be rather different. Furthermore, there exist cases, e.g., the location of the weak interface makes a big difference in the slope of the straight solid line without any markers in Fig. 2 and 3 for $\Delta\omega_{(1)}$ and $\Delta\omega_{(2)}$. Such a characteristic can be used to determine the location of the weak interface. For example, we can measure the frequency shifts of the first two frequencies of the structure, and compare the ratio with the slopes in the two figures to see which one is closer to the measured result. In such a way, the imperfect interface may be located easily. Of course, if the location of the weak interface dose not make big difference between the ratios of the frequency shifts of the two chosen modes, e.g., the solid line with solid square markers in Figs. 2 and 3 for $\Delta\omega_{(1)}$ and $\Delta\omega_{(3)}$, then it is difficult for us to determine the damage location since the measured result is close to both analytical results. When this situation happens, we can try to make use of high-order frequencies, or explore vibration modes other than the TSh.

Finally we note that the data points in Figs. 2 and 3 as calculated from Eqs. (28) and (31) fall into straight lines exactly as shown only when S_1 (or S_2) is small (of the order 10^{-17} m^3/N). When S_1 (or S_2) is not small, frequency shifts cannot be expressed in the form of (25) and need to be calculated directly from Eq. (14). In that case calculations show that frequency shifts deviate the straight lines shown in Figs. 2 and 3.

7. Conclusions

When one of the two interfaces in a three-layered plate is slightly weakened as described by the shear-lag model, TSh modes of different orders feel the weakened interface differently, resulting in different frequency shifts. Frequency shifts of two specific modes are proportional, and the proportionality depends on which interface is weakened. This provides a potential way for locating the specific weak interface. The approach in this paper may be generalized to other modes like thickness-stretch in plates, plates with more than three layers, or weak interfaces described by other models.

Acknowledgements

The work was supported by the NSFC (Nos. 11102183, 10832009 and 10725210) and the National Basic Research Program of China (No. 2009CB623200).

References

Accuratus Corporation, "Fused Silica, SiO_2 Material Properties", http://accuratus.com/fused.html, 2012-02-02.

Chen, W.Q., Cai, J.B. and Ye, G.R. (2003), "Exact solutions of cross-ply laminates with bonding imperfections", *AIAA J.*, **41**(11), 2244-2250.

Chen, W.Q., Cai, J.B. and Ye, G.R. (2005), "Responses of cross-ply laminates with viscous interfaces in cylindrical bending," *Comput. Meth. Appl. M.*, **194**(6-8), 823-835.

Chen, W.Q., Wang, Y.F., Cai, J.B. and Ye, G.R. (2004), "Three-dimensional analysis of cross-ply laminated cylindrical panels with weak interfaces", *Int. J. Solids Struct.*, **41**(9-10), 2429-2446.

Chen, Y.J., Shib, Y.W. and Zhang, X.P. (1998), "Detection of weak bonding in friction welds by ultrasound", *Ultrasonics*, **36**(1-5), 141-146.

Cheng, Z.Q., Kennedy, D. and Williams, F.W. (1996), "Effect of interfacial imperfection on buckling and bending behavior of composite laminates", *AIAA J.*, **34**(12), 2590-2595.

Di Sciuva, M. (1997), "Geometrically nonlinear theory of multilayered plates with interlayer slips", *AIAA J.*,

35(11), 1753-1759.

Fan, H., Yang, J.S. and Xu, L.M. (2006), “Piezoelectric waves near an imperfectly bonded interface between two half-spaces”, *Appl. Phys. Lett.*, **88**(20), 203509.

Friswell, M.I. (2007), “Damage identification using inverse methods”, *Phil. Trans. R. Soc. A.,* **365**(1851), 393-410.

Friswell, M.I. and Mottershead, J.E. (2001), “Inverse methods in structural health monitoring”, *Key Eng. Mat.*, **204-205**, 201-210.

Icardi, U., Di Sciuva, M. and Librescu, L. (2000), “Dynamic response of adaptive cross-ply cantilevers featuring interlaminar bonding imperfections”, *AIAA J.*, **38**(3), 499-506.

Jin, F., Kishimoto, K., Inoue, H. and Tateno, T. (2005), “Experimental investigation on the interface properties evaluation in piezoelectric layered structures by loves waves propagation”, *Key Eng. Mat.*, **297-300**, 807-812.

Kumar, R. and Singh, M. (2009), “Effect of rotation and imperfection on reflection and transmission of plane waves in anisotropic generalized thermoelastic media”, *J. Sound Vib.*, **324**(3-5), 773-797.

Li, F.M., Wang, Y.Z., Fang, B. and Wang, Y.S. (2007), “Propagation and localization of two- dimensional in-plane elastic waves in randomly disordered layered piezoelectric phononic crystals”, *Int. J. Solids Struct.*, **44**(22-23), 7444-7456.

Librescu, L. and Schmidt, R. (2001), “A general linear theory of laminated composite shells featuring interlaminar bonding imperfections”, *Int. J. Solids Struct.*, **38**(19), 3355-3375.

Lu, X. and Liu, D. (1992), “Interlaminar shear slip theory for cross-ply laminates with non-rigid interfaces”, *AIAA J.*, **30**(4), 1063-1073.

Piskunov, V.G. and Rasskazov, A.O. (2002), “Evolution of the theory of laminated plates and shells”, *Int. Appl. Mech.*, **38**(2), 135-166.

Reddy, J.N. (2004), *Mechanics of Laminated Composite Plates and Shells: Theory and Analysis*, CRC Press, Boca Raton.

Rinker, B.A., Jamieson, E.E., Samayoa, J.A., Abeln, T.G., Lerch, T.P. and Neal, S.P. (2003), “Detection of weak interface signals for same material bond/weld inspection”, *AIP Conf. Proc.*, **657**(1), 1080-1087.

Shu, X.P. (2001), “Vibration and bending of antisymmetrically angle-ply laminated plates with perfectly and weakly bonded layers”, *Compos. Struct.*, **53**(2), 245-255.

Tomar, S.K. and Gogna, M.L. (1995), “Reflection and refraction of longitudinal wave at an interface between two micropolar elastic solids in welded contact”, *J. Acoust. Soc. Am.,* **97**(2), 822-830.

Tsubouchi, K., Sugai, K. and Mikoshiba, N. (1981), “AlN material constants evaluation and SAW properties on AlN/Al_2O_3 and AlN/Si”, *IEEE Ultrasonics Symp.*, 375-380.

Wang, Y.Z., Li, F.M., Huang, W.H. and Wang, Y.S. (2008), “The propagation and localization of Rayleigh waves in disordered piezoelectric phononic crystals”, *J. Mech. Phys. Solids*, **56**(4), 1578-1590.

Wang, Y.Z., Li, F.M., Kishimoto, K., Wang, Y.S. and Huang, W.H. (2010), “Wave localization in randomly disordered layered three-component phononic crystals with thermal effects”, *Arch. Appl. Mech.*, **80**(6), 629-640.

Yang, J.S., Hu, Y.T., Zeng, Y. and Fan, H. (2006), “Thickness-shear vibration of rotated Y-cut quartz plates with imperfectly bonded surface mass layers”, *IEEE Trans. Ultrason. Ferroelect. Freq. Contr.*, **53**(1), 241-245.

Yang, S., Gu, L. and Gibson R.F. (2001), “Nondestructive detection of weak joints in adhesively bonded composite structures”, *Compos. Struct.*, **51**(1), 63-71.